THE JOURNAL OF PHYSICAL CHEMISTRY A

pubs.acs.org/JPCA Article

Improving Excited-State Potential Energy Surfaces via Optimal Orbital Shapes

Lan Nguyen Tran* and Eric Neuscamman*

Cite This: J. Phys. Chem. A 2020, 124, 8273–8279 Read Online

ACCESS | Metrics & More | Article Recommendations

ABSTRACT: We demonstrate that, rather than resorting to high-cost dynamic correlation methods, qualitative failures in excited-state potential energy surface predictions can often be remedied at no additional cost by ensuring that optimal molecular orbitals are used for each individual excited state. This approach also avoids the weighting choices required by state-averaging and dynamic weighting and obviates their need for expensive wave function response calculations when relaxing excited-state geometries. Although multistate approaches are of course preferred near conical intersections, other features of excited-state potential energy surfaces can benefit significantly from our single-state approach. In three different systems, including a double bond dissociation, a biologically relevant amino hydrogen dissociation, and an amino-to-ring intramolecular charge transfer, we show that state-specific orbitals offer qualitative improvements over the state-averaged status quo.

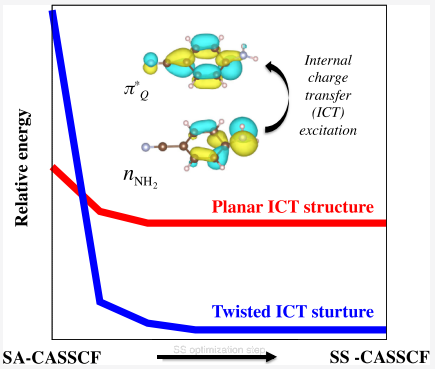

1. INTRODUCTION

Exited-state geometry relaxations are an essential phenomenon in molecular photochemistry. Alongside inter-state properties such as nonadiabatic couplings and transition dipoles, single-state potential energy surface (PES) features such as the depths and locations of excited-state minima and the heights of barriers between minima help determine how a molecule will respond and transform under exposure to light. For example, selecting ligands in order to extend the lifetimes of Fe-based metal-to-ligand charge-transfer (MLCT) states depends centrally on the relative energies and positions of MLCT and other excited state minima.[1−5] While density functional theory (DFT), with its low-cost and often excellent ground state energetics, is widely used in studying excited states, its well-known difficulties with charge-transfer states and in systems exhibiting strong electron correlations make reliable, low-cost alternatives a high priority in the study of photochemistry. The complete active space self-consistent field (CASSCF) approach is often a powerful alternative,[6−8] but it is significantly more difficult to use than DFT and, due to its own limitations, can still make qualitative errors in PESs without the aid of expensive post-CASSCF correlation corrections. A good example of this frustrating reality occurs in the charge-transfer state of 4-aminobenzonitrile (ABN), where state-averaging compromises prevent the wave function from undergoing proper orbital relaxation and lead CASSCF to predict a qualitatively incorrect excited state geometry.[9] Although applying corrections with complete active space perturbation theory (CASPT2) brings predictions in line with the experiment,[9] such post-CASSCF correlation methods greatly increase computational cost. While such methods' incorporation of the finer details of electron correlation is essential for high-precision energetics, we show here that in this case and others, qualitatively correct predictions can be restored simply by making the molecular orbital shapes optimal for individual excited states.

While the widely used practice of state-averaging (SA) has seen many successes in excited state investigations, it faces a number of important challenges. In the SA approach, the molecular orbital shapes are chosen by minimizing the weighted average of multiple states' energies. This appears at first glance to be balanced, and in many cases is, but can also entrench imbalances if the needs of one state (e.g., strong orbital relaxations following charge transfer) are denied in favor of the needs of others (e.g., multiple local excitations that should not involve strong orbital relaxations). As we discuss below, this problem appears to be responsible for SA-CASSCF's failure to predict an excitation-induced twist in ABN. SA-CASSCF is also a popular way to address the challenge of root flipping, where an optimization fails to converge due to two states exchanging back and forth in the energy ordering. However, SA is not a panacea here, as there is always the risk of the highest-energy state in the average flipping with the next state not included in the average. Glover, for example, has recently shown explicitly that SA-

Received: August 20, 2020
Published: September 4, 2020

https://dx.doi.org/10.1021/acs.jpca.0c07593
J. Phys. Chem. A 2020, 124, 8273–8279

CASSCF still suffers from root flipping.[10] Another challenge is that SA-CASSCF often introduces discontinuities in PESs,[10−13] which can be a particular problem for dynamics simulations.[10,14] Whether these discontinuities arise from the highest state in the average crossing the lowest state not in the average as the atoms move around or from a cusp in a single state being converted to a discontinuity in all states via the SA link, this high-priority problem has attracted a good deal of attention. One approach to address the issue is to prepare good orbital sets for complete active space configuration interaction (CASCI), such as floating occupation molecular orbitals,[15] and then forgoing the SA-CASSCF orbital optimization entirely. While less prone to PES discontinuities, this approach unfortunately can still produce them for high-lying excited states.[16] An alternative approach, and one that is particularly relevant near conical intersections where retaining at least a two-state treatment is advantageous, is to weigh the SA dynamically so as to favor the needs of the important states while retaining the stability offered by SA.[10−12] The drawback is that the now energy-dependent weights complicate the evaluation of analytic gradients even more than SA does already.[10,12] In principle, discontinuities and root flipping could be avoided if one were able to enlarge the active space to a sufficient degree. This can be expensive in practice, however, even with modern methods for large active spaces, such as density matrix renormalization group[17,18] and stochastic-based configuration interaction methods.

Seeking to avoid these difficulties, we have recently developed a new state-tracking method in order to facilitate excited-state-specific orbital optimization.[13] We demonstrated that our method is more effective for state-specific optimization than either the naive simple root selection (SRS) based on energy ordering or a direct generalization of the maximum overlap method based on CI vectors. We also showed that state-specific CASSCF (SS-CASSCF) is a better reference for perturbation theory than SA-CASSCF, especially for charge-transfer states. In this paper, rather than single-point calculations, we generalize our approach to describe PESs. We will show how SS-CASSCF can succeed in cases where SA-CASSCF suffers qualitative failures. In addition to the case of ABN, where experiment and expensive post-CASSCF methods predict a twisted charge-transfer geometry while SA-CASSCF does not,[19,20] we investigate the crossing of aniline's first $^1\pi\pi^*$ and charge-transfer states (which SA-CASSCF fails to predict[21,22]) and PES disappearance and discontinuity in thioacetone. In addition to qualitative improvements in accuracy, it is important to emphasize that the excited-state-specific approach, by making the state's energy stationary with respect to the orbital shapes, avoids the response calculations that SA-CASSCF and dynamic weighting need to perform[23] when evaluating analytic gradients. Avoiding the response evaluations matters, as they are more expensive[24] and can be more prone to convergence issues[25] than CASSCF itself. In our approach, analytic gradients are no more difficult than in the ground state case and indeed can use the exact same gradient code. While these advantages in both accuracy and numerical simplicity are exciting, we should keep in mind that SA-CASSCF is popular precisely because it is often successful, and so it is important to emphasize the particular situations in which it is most in need of assistance. In this regard, we will point to charge transfer, which is a technologically important case where SA is at particular risk of entrenching biases between states rather than creating balance.[13,26,27]

2. THEORY

Our state-specific approach (SS-CASSCF) rests on the general property that exact Hamiltonian eigenstates are energy stationary points. In the context of an approximate ansatz-like CASSCF, the idea is to find the ansatz's stationary point that corresponds to the excited state under study. For simplicity, we retain the two-step approach common to many CASSCF implementations in which the orbitals and CI variables are optimized separately. In particular, the orbitals are optimized so as to minimize the energy gradient norm[13] (rather than the energy, which would encourage collapse towards the ground state), while the CI variables are chosen at each stage as the CASCI root most similar to the desired state. While there are of course many ways to make a precise definition for what one means by similar, we have found[13] that the measure

$$Q_{\mathrm{W}\Gamma} = \frac{\langle\Psi|(\omega - \hat{H})^2|\Psi\rangle}{\langle\Psi|\Psi\rangle} + \frac{||\Gamma_t - \Gamma||}{n_{\mathrm{CAS}}} \tag{1}$$

is particularly effective. Here, ω is a target energy that we think is close to the energy of the state we are after, Γ is our state's one-body density matrix, Γ_t is a target density matrix (taken either from an initial CASCI or from the previous iteration), and n_{CAS} is the number of active orbitals. The idea is that, after finding the low-energy roots of the CASCI problem, we select the root with the lowest value for $Q_{\mathrm{W}\Gamma}$ and then perform an orbital optimization step that seeks to make that root's energy stationary with respect to orbital changes. Crucially, the selection of the root based on its energy and density matrix makes the approach insensitive to root flipping, so even in cases where the order of the states in the CASCI changes as the orbitals are optimized, the approach converges to the energy stationary point corresponding to the desired excited state.[13] Note especially that the precise choices for ω and Γ_t do not affect the final outcome so long as they lead the optimization to converge to the correct CASSCF stationary point. In other words, the final energy depends only on the wave function at the energy stationary point, which is independent of ω and Γ_t, but made easier to find and converge to via intelligent choices for these parameters.

Once the energy is stationary, the Hellman−Feynman theorem guarantees that analytic gradients with respect to nuclear coordinates R simplify to

$$\frac{\mathrm{d}E}{\mathrm{d}R} = \left\langle \Psi \middle| \frac{\partial \hat{H}}{\partial R} \middle| \Psi \right\rangle \tag{2}$$

in a direction parallel to the situation for ground states. There is no need for response calculations, as full energy stationary eliminates the wave function response terms from the gradient expression. In SA-CASSCF, in contrast, the energies of individual states that control the PES are not stationary (it is only their weighted average that is) and so additional terms involving the wave function's response to the geometry distortion appear in the gradient equation and must be evaluated. Our analytic gradients in hand, we perform our geometry relaxations using the *geomopt* module within pySCF,[28] which interfaces with geomeTRIC[29] and PyBerny[30] for constrained and unconstrained geometry optimizations, respectively. Comparison calculations with SA-CASSCF were performed using Molpro.[31]

https://dx.doi.org/10.1021/acs.jpca.0c07593
J. Phys. Chem. A 2020, 124, 8273−8279

3. RESULTS AND DISCUSSION

Let us begin with the relatively simple example of C−S bond photodissociation, which can be important in astrochemistry,[32] biomedicine,[33] and catalysis.[34] For C−S single bond dissociation, nonradiative internal conversion between the first excited state $^1\pi\pi^*$ and the dissociative $^1\pi\sigma^*$ state is key.[35] Here, we instead investigate the C−S double bond dissociation of thioacetone, $(CH_3)_2CS$, using both SA-CASSCF and SS-CASSCF. By performing geometry relaxations for each of the low-lying singlet states at a series of fixed C−S bond distances, we can see which states are expected to be key for the double bond dissociation. We see in Figure 1 that, among the low-lying

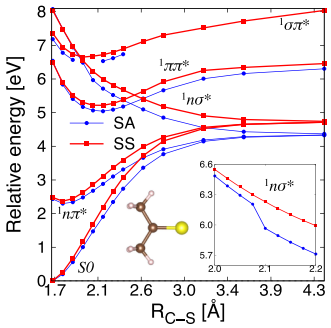

Figure 1. Potential energy curves showing, for each low-lying singlet state of thioacetone, the energy of the state after relaxing the geometry with the C−S bond distance R_{C-S} held fixed. SA-CASSCF used a 5-state SA with equal weights, while both SA-CASSCF and SS-CASSCF employed the 6-31G(d) basis and a (6e,5o) active space containing the σ, σ^*, π, π^*, and lone pair n orbitals.

singlets, it is the $^1n\sigma^*$ state that is dissociative in character, while the $^1n\pi^*$, $^1\pi\pi^*$, and $^1\sigma\pi^*$ surfaces are all bound. For the lowest four states, the SA and SS approaches are in qualitative agreement, but SS-CASSCF displays a clear advantage for the $^1\sigma\pi^*$ state. For this state, the SA-CASSCF geometry optimization was unable to converge at most C−S bond distances, while SS-CASSCF optimizations converged at all distances. While it is possible that extending the SA to include more than five states could help here, this is highly undesirable, as including more states leads to each state having even less say in how the orbitals should be shaped and, worse, increases the chances of finding discontinuities, as a discontinuity in any states' surface gets spread to all states through their link in the SA energy. With five states in the average, SA-CASSCF suffers one discontinuity already, as the inset of Figure 1 shows, which is near the R_{C-S} = 2.1 Å geometry of the $^1n\sigma^*$ state. (Note that, although at that geometry all states show a discontinuity due to the SA link, this is not seen in the figure, as the other states' energies are being reported at their own relaxed geometries.) The discontinuity is relatively small and does not alter the basic dissociative character of the state, but even small discontinuities can strongly affect dynamics simulations.[10,12] In the SS approach, in contrast, the $^1\sigma\pi^*$ and $^1n\sigma^*$ states are quite well behaved, and we need not agonize over how many states to include in any average and how this may affect orbital quality. With the molecular orbital shapes now optimal for each state individually, these difficulties are avoided, the geometry optimizations all converge successfully, and no discontinuities are encountered.

We now turn our attention to aniline, $(C_6H_5NH_2)$, a common basis unit for biomolecules whose N−H photodissociation is important for medical applications, including UV radiation protection within sunscreen.[36] Aniline's excited-state dynamics have been extensively studied,[21,22,36−40] and as is common for heteroaromatic biomolecules, the $^1\pi\sigma^*$ state has been shown to facilitate the photodissociation process.[36] In Figure 2, we plot

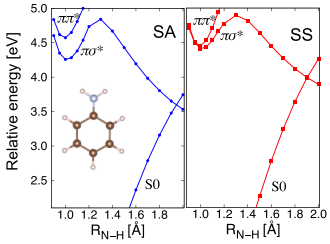

Figure 2. Potential energy curves showing, for three low-lying singlet states of aniline, the energy of the state after relaxing its geometry under C_s symmetry with the N−H bond distance R_{N-H} held fixed. SA-CASSCF used a 3-state SA with equal weights, while both SA-CASSCF and SS-CASSCF employed the 6311++g(d,p) basis and a (10e,9o) active space containing seven π/π^* orbitals, an N−H σ orbital, and an N−H σ^* orbital.

PESs for the three lowest singlet states after relaxing their geometries with one N−H bond length held fixed. Both SA- and SS-CASSCF show that the $^1\pi\sigma^*$ state is quasi-bound in the region of the S0 minimum, with dissociative character only appearing once the N−H bond has been stretched. A previous theoretical investigation using the equation of motion coupled cluster model with single and double substitutions (EOM-CCSD) predicts the barrier to leave the quasi-bound region and dissociate to be 0.5 eV.[39] We note that, although it is a small advantage, the SS-CASSCF dissociation barrier of 0.49 eV is closer to the 0.5 eV EOM-CCSD prediction[39] than is the 0.58 eV barrier of SA-CASSCF.

Experimental investigations suggest that the first $^1\pi\pi^*$ excited state intersects the $^1\pi\sigma^*$ state near the latter's quasi-bound local minimum geometry.[37] Previous theoretical investigation has failed to predict this crossing using SA-CASSCF,[21,22] and it is only when expensive post-CASSCF methods such as extended multiconfiguration quasi-degenerate second-order perturbation theory[21] (XMC-QDPT2) and extended multi-state multi-reference perturbation theory[22] (XMS-CASPT2) are employed that a crossing is predicted. With the $^1\pi\sigma^*$ state showing a substantial change in dipole moment compared to the ground state and thus possessing at least some charge-transfer character, we wondered whether predicting the crossing really required such expensive methodology or, instead, whether this was a case in which states with substantially different needs in terms of molecular orbital shapes were being ill-served by the compromises inherent to SA. To this end, in Figure 3, we plot PESs of these two excited states along the N−H bond dissociation with all other coordinates held fixed at the SS-CASSCF ground state minimum. Dynamical correlation missing at the CASSCF level is considered using CASPT2. For comparison, EOM-CCSD's PESs are also plotted. Both single-state CASPT2 calculations using SA- and SS-CASSCF references (SA-CASPT2 and SS-CASPT2, respectively) predict crossings near an N−H distance of 1.25 Å. It is noteworthy that while SA- and SS-CASPT2 PESs of the valence $\pi\pi^*$ state are very similar, those of the charge-transfer $\pi\sigma^*$ state are meaningfully different (the SA one is deeper than the SS one), showing that state-specific orbital optimization effects can carry

https://dx.doi.org/10.1021/acs.jpca.0c07593
J. Phys. Chem. A 2020, 124, 8273−8279

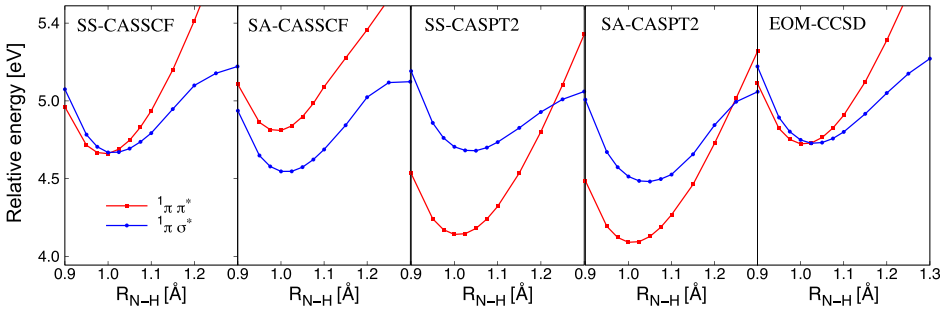

Figure 3. Potential energy curves of the two lowest singlet excited states of aniline along the N−H bond dissociation with all other coordinates held fixed at the SS-CASSCF ground-state minimum. SS-CASSCF, single-state CASPT2, and EOM-CCSD predict a crossing, while SA-CASSCF does not.

over to post-CASSCF methods. More importantly, we see that SA-CASSCF fails to predict a crossing, whereas SS-CASSCF predicts a crossing near an N−H bond distance of 1.05 Å. Although the crossing distance predicted by SS-CASSCF is shorter than that of CASPT2 (post-CASSCF correlation effects do play a quantitative role here), the fact that SS-CASSCF predicts a crossing at all is a qualitative improvement over the SA approach. A final interesting point here is that SS-CASSCF makes a very similar prediction as EOM-CCSD, despite being a significantly less expensive method.

To understand why SA-CASSCF has difficulty here, we have plotted the σ^* orbital from our SS-CASSCF $^1\pi\sigma^*$ state in Figure 4, where we see that the charge-transfer character suggested by

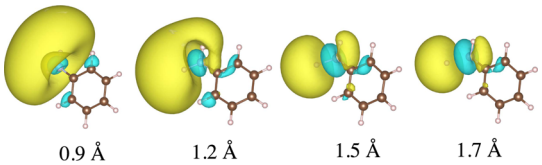

Figure 4. σ^* orbital of aniline in the SS-CASSCF $^1\pi\sigma^*$ state at various N−H bond distances.

the large dipole change is really a Rydberg-like extension of the σ^* orbital off one side of the molecule. The large change in dipole is nonetheless present, which creates a state-specific need for the nonactive orbitals to respond and repolarize their electron distributions. This effect is difficult to achieve in SA-CASSCF, as these repolarizations are inappropriate for the other two states. We find that, even if we use a biased S0/$\pi\sigma^*$/$\pi\pi^*$ weighting of 20/40/40, the excited state energies do not get closer together. This finding strongly suggests that dynamic weighting would not help here, which is not surprising as, again, the issue is that the two states have significantly different dipoles and so require different postexcitation orbital relaxations. By instead going in for fully state-specific orbitals, which can be seen as the logical endpoint of biased weighting, the different states get the orbital relaxations that are appropriate to them, and a crossing is successfully predicted.

Finally, we consider intramolecular charge transfer (ICT) in ABN, where Segado and co-workers have shown[9] that SA-CASSCF predicts a qualitatively incorrect structure for the minimum-energy geometry of the ICT state. In addition to a normal fluorescence band associated with a locally excited (LE) state, UV excitation of this molecule also produces an anomalous fluorescence band due to emission from the ICT state.[19,20] As shown in Figure 5, there are multiple local minima on the ICT surface that could in principle be relevant. In the planar (PICT) geometry, the amino group, the benzene ring, and the cyano

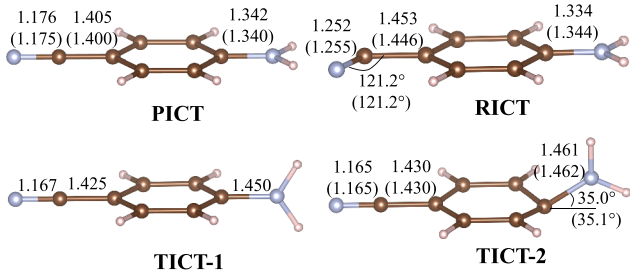

Figure 5. SS-CASSCF local minima on the ICT surface of ABN, with corresponding SA-CASSCF values reported from Segado and co-workers[9] given in parentheses. Both approaches used the cc-pVDZ basis set and a (12e,11o) active space that contains the benzene π and π^* orbitals, the amino nitrogen lone pair, and the four π and π^* orbitals of the cyano group.

group all lie in the same plane.[41] In the rehybridized (RICT) geometry, the cyano group is wagged in the plane of the ring due to a rehybridization of the cyano carbon atom from sp to sp^2.[42,43] In the twisted (TICT) geometries, the amino group is rotated so that its plane is (almost) perpendicular to that of the ring[19,44] and may (TICT-1) or may not (TICT-2) involve the group's bond to the ring lying in the ring's plane.[9] While the experiment and high-cost post-CASSCF methods agree that the most stable geometry is twisted,[19,20] Segado and co-workers have shown that SA-CASSCF instead predicts the fully planar geometry to be more stable by almost 15 kcal/mol.[9] As in aniline, this system involves states for which the appropriate postexcitation orbital relaxations differ significantly, and so it is again worth asking whether qualitatively correct predictions really do require expensive post-CASSCF methods or simply that each state be able to enjoy molecular orbitals that have been optimized to suit its needs.

Although Figure 5 reveals that the structures predicted by SS-CASSCF agree with those from SA-CASSCF, Table 1 shows that the energetics are quite different and that, as anticipated, state-specific orbital relaxation leads to predictions that agree qualitatively with the experiment and post-CASSCF methods. In particular, SS-CASSCF agrees with MS-CASPT2 in predicting that TICT-2 is the most stable ICT structure.[9] By allowing orbitals to fully relax following the charge transfer, SS-CASSCF stabilizes the ICT state at all geometries, but the effect is much stronger in the twisted geometries, as shown, for example, in Figure 6. These results imply that the SA compromise for orbital shapes, which is always worrisome when the noncharge-transfer states (S0, LE) outnumber charge-transfer states (ICT), creates a significantly stronger bias against the ICT state at some geometries than at others, ruining the balance that SA is in

https://dx.doi.org/10.1021/acs.jpca.0c07593
J. Phys. Chem. A 2020, 124, 8273−8279

Table 1. Energy Differences ΔE Relative to the S0 Minimum (in kcal/mol) and Dipoles (in debye) for ABN's ICT State at Different Minima on Its PES for Our SS-CASSCF, the 3-State SA-CASSCF, and MS-CASPT2 Approaches of Segado and Co-workers[9]

	SS-CASSCF		SA(3)-CASSCF[9]		MS-CASPT2[9]	
states	ΔE	μ	ΔE	μ	ΔE	μ
S0	0	6.08	0	5.40	0	
PICT	139.19	11.92	146.15	11.23	116.99	
RICT	140.50	13.95	152.77	10.45	122.14	
TICT-1	131.70	13.66				
TICT-2	128.02	10.66	160.93	10.76	110.16	

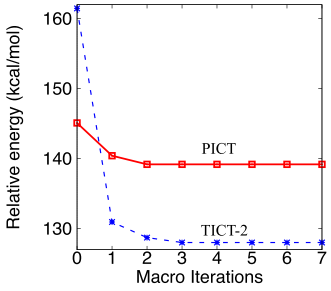

Figure 6. As an example of how much the SA bias against the ABN's ICT state varies with geometry, we plot the lowering of this state's energy during SS-CASSCF optimizations that start from the SA-CASSCF wave functions at both the SS-CASSCF planar (PICT) and twisted (TICT-2) geometries. Energies are reported relative to the S0 minimum.

principle supposed to provide. In contrast, our root-tracking method's ability to tailor orbitals for individual states without losing track of those states during the wave function optimization (see Figure 7, which also shows that SRS fails to

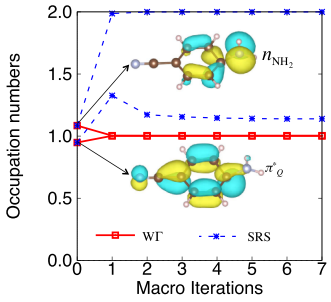

Figure 7. Orbital occupation changes during SS-CASSCF's wave function optimization of the ABN's ICT state at the TICT-2 geometry, with SA-CASSCF used as the guess. Our WΓ approach maintains the correct state character,[9] whereas SRS, which selects the CASCI root based on energy ordering, collapses to a noncharge-transfer state.

converge to the correct state here, making this a case where our new approach to SS-CASSCF makes the difference) allows for the energetically significant repolarizations that all orbitals are expected to undergo following a charge transfer. Interestingly, capturing these effects is sufficient to bring the prediction in line with experiment, again suggesting that one can go a long way in repairing the failures of SA-CASSCF without resorting to the expense of post-CASSCF methods. When one considers that this should be especially true in charge-transfer systems and that, in order to separate charges over a significant distance for technological purposes, these systems often contain dozens or even hundreds of atoms, and the advantages of improving accuracy without increasing cost become even more desirable.

4. CONCLUSIONS

In summary, we have shown that by providing each excited state with orbitals that are optimal for its needs, qualitative failures in PESs can be corrected without significantly increasing computational cost. Moreover, state-specific orbitals dramatically simplify the evaluation of analytic gradients by eliminating the wave function response calculations that are required by state-averaged approaches. In particular, we have shown that this state-specific approach, in which collapse to other states is avoided via novel root tracking, makes qualitative improvements over SA in a C−S double bond dissociation, in an amino N−H dissociation, and in an ICT geometry relaxation. Our approach's general nature—it requires the same basic ingredients as can be found in ground state CASSCF implementations—should allow these advantages to be enjoyed across a wide variety of excited state applications, with particular promise for cases such as charge transfer and core excitation that involve substantial postexcitation orbital relaxation.

Looking forward, there are a number of clear ways in which the methodology can be enhanced to further widen its utility. Thanks to its two-step optimization formulation, it should be quite straightforward to tackle large active spaces with selective CI or the density matrix renormalization group. Combining these approaches with excited-state-specific orbital relaxations looks especially promising for MLCT complexes, where double-d-shell effects and large ligand π systems quite rapidly push the desired active space beyond the reach of conventional solvers. A second obvious priority is enabling interstate properties such as transition dipoles and derivative couplings. Although our approach leads naturally to a situation in which different states are expressed in different molecular orbital bases and so makes inter-state matrix elements less straightforward, non-orthogonal configuration interaction techniques can be adapted to meet this challenge. These same techniques are also relevant for rediagonalizing a pair of states near a conical intersection, where the lack of strict orthogonality within our state-specific approach becomes a real concern. With these various improvements, it should be possible to bring the benefits of state-specific orbital optimization and the qualitative improvements in accuracy that it offers to the wide array of property predictions on which spectroscopists depend.

AUTHOR INFORMATION

Corresponding Authors

Lan Nguyen Tran − *Department of Chemistry, University of California, Berkeley, California 94720, United States; Ho Chi Minh City Institute of Physics, VAST, Ho Chi Minh City 700000, Vietnam;* orcid.org/0000-0003-2649-2122; Email: lantrann@berkeley.edu

Eric Neuscamman − *Department of Chemistry, University of California, Berkeley, California 94720, United States; Chemical Sciences Division, Lawrence Berkeley National Laboratory, Berkeley, California 94720, United States;* orcid.org/0000-0002-4760-8238; Email: eneuscamman@berkeley.edu

Complete contact information is available at: https://pubs.acs.org/10.1021/acs.jpca.0c07593

Notes

The authors declare no competing financial interest.

https://dx.doi.org/10.1021/acs.jpca.0c07593
J. Phys. Chem. A 2020, 124, 8273−8279

■ ACKNOWLEDGMENTS

This work was supported by the Early Career Research Program of the Office of Science, Office of Basic Energy Sciences, the U.S. Department of Energy, grant no. DE-SC0017869. Calculations ran on the Berkeley Research Computing Savio cluster.

■ REFERENCES

(1) de Graaf, C.; Sousa, C. Study of the light-induced spin crossover process of the [FeII (bpy) 3] 2+ complex. *Chem.—Eur. J.* **2010**, *16*, 4550.
(2) Graaf, C. D.; Sousa, C. On the role of the metal-to-ligand charge transfer states in the light-induced spin crossover in FeII (bpy)3. *Int. J. Quantum Chem.* **2011**, *111*, 3385.
(3) Zhang, W.; Kjær, K. S.; Alonso-Mori, R.; Bergmann, U.; Chollet, M.; Fredin, L. A.; Hadt, R. G.; Hartsock, R. W.; Harlang, T.; Kroll, T.; et al. Manipulating charge transfer excited state relaxation and spin crossover in iron coordination complexes with ligand substitution. *Chem. Sci.* **2017**, *8*, 515.
(4) Wenger, O. S. Is iron the new ruthenium? *Chem.—Eur. J.* **2019**, *25*, 6043.
(5) Wu, J.; Alías, M.; de Graaf, C. Controlling the Lifetime of the Triplet MLCT State in Fe (II) Polypyridyl Complexes through Ligand Modification. *Inorganics* **2020**, *8*, 16.
(6) González, L.; Escudero, D.; Serrano-Andrés, L. Progress and challenges in the calculation of electronic excited states. *ChemPhysChem* **2012**, *13*, 28.
(7) Aquilante, F.; Pedersen, T. B.; Veryazov, V.; Lindh, R. MOLCAS-a software for multiconfigurational quantum chemistry calculations. *WIRE Comput. Mol. Sci.* **2013**, *3*, 143.
(8) Serrano-Andrés, L.; Merchán, M. Quantum chemistry of the excited state: 2005 overview. *J. Mol. Struct.: THEOCHEM* **2005**, *729*, 99.
(9) Segado, M.; Gómez, I.; Reguero, M. Intramolecular charge transfer in aminobenzonitriles and tetrafluoro counterparts: fluorescence explained by competition between low-lying excited states and radiationless deactivation. Part I: A mechanistic overview of the parent system ABN. *Phys. Chem. Chem. Phys.* **2016**, *18*, 6861.
(10) Glover, W. J. Communication: Smoothing out excited-state dynamics: Analytical gradients for dynamically weighted complete active space self-consistent field. *J. Chem. Phys.* **2014**, *141*, 171102.
(11) Deskevich, M. P.; Nesbitt, D. J.; Werner, H.-J. Dynamically weighted multiconfiguration self-consistent field: Multistate calculations for F+ H 2 O → HF+ OH reaction paths. *J. Chem. Phys.* **2004**, *120*, 7281.
(12) Glover, W. J.; Paz, A. S. P.; Thongyod, W.; Punwong, C. Analytical gradients and derivative couplings for dynamically weighted complete active space self-consistent field. *J. Chem. Phys.* **2019**, *151*, 201101.
(13) Tran, L. N.; Shea, J. A. R.; Neuscamman, E. Tracking excited states in wave function optimization using density matrices and variational principles. *J. Chem. Theory Comput.* **2019**, *15*, 4790.
(14) Hollas, D.; Šištík, L.; Hohenstein, E. G.; Martínez, T. J.; Slavíček, P. Nonadiabatic ab initio molecular dynamics with the floating occupation molecular orbital-complete active space configuration interaction method. *J. Chem. Theory Comput.* **2018**, *14*, 339.
(15) Slavíček, P.; Martínez, T. J. Ab initio floating occupation molecular orbital-complete active space configuration interaction: An efficient approximation to CASSCF. *J. Chem. Phys.* **2010**, *132*, 234102.
(16) Yang, J.; Zhu, X.; Wolf, T. J. A.; Li, Z.; Nunes, J. P. F.; Coffee, R.; Cryan, J. P.; Gühr, M.; Hegazy, K.; Heinz, T. F.; et al. Imaging CF3I conical intersection and photodissociation dynamics with ultrafast electron diffraction. *Science* **2018**, *361*, 64−67.
(17) Chan, G. K.-L.; Sharma, S. The density matrix renormalization group in quantum chemistry. *Annu. Rev. Phys. Chem.* **2011**, *62*, 465.
(18) Hu, W.; Chan, G. K.-L. Excited-state geometry optimization with the density matrix renormalization group, as applied to polyenes. *J. Chem. Theory Comput.* **2015**, *11*, 3000.
(19) Grabowski, Z. R.; Rotkiewicz, K.; Rettig, W. Structural changes accompanying intramolecular electron transfer: focus on twisted intramolecular charge-transfer states and structures. *Chem. Rev.* **2003**, *103*, 3899.
(20) Misra, R.; Bhattacharyya, S. P. *Intramolecular Charge Transfer: Theory and Applications*; John Wiley & Sons, 2018.
(21) Sala, M.; Kirkby, O. M.; Guérin, S.; Fielding, H. H. New insight into the potential energy landscape and relaxation pathways of photoexcited aniline from CASSCF and XMCQDPT2 electronic structure calculations. *Phys. Chem. Chem. Phys.* **2014**, *16*, 3122.
(22) Ray, J.; Ramesh, S. G. Conical intersections involving the lowest $1\pi\sigma^*$ state in aniline: Role of the NH2 group. *Chem. Phys.* **2018**, *515*, 77.
(23) Yamaguchi, Y. *A New Dimension to Quantum Chemistry: Analytic Derivative Methods in Ab Initio Molecular Electronic Structure Theory*; Oxford University Press: USA, 1994.
(24) Granovsky, A. A. Communication: An efficient approach to compute state-specific nuclear gradients for a generic state-averaged multi-configuration self consistent field wavefunction. *J. Chem. Phys.* **2015**, *143*, 231101.
(25) Dudley, T. J.; Olson, R. M.; Schmidt, M. W.; Gordon, M. S. Parallel coupled perturbed CASSCF equations and analytic CASSCF second derivatives. *J. Comput. Chem.* **2006**, *27*, 352.
(26) Domingo, A.; Carvajal, M. À.; de Graaf, C.; Sivalingam, K.; Neese, F.; Angeli, C. Metal-to-metal charge-transfer transitions: reliable excitation energies from ab initio calculations. *Theor. Chem. Acc.* **2012**, *131*, 1264.
(27) Pineda Flores, S. D.; Neuscamman, E. Excited State Specific Multi-Slater Jastrow Wave Functions. *J. Phys. Chem. A* **2019**, *123*, 1487−1497.
(28) Sun, Q.; Berkelbach, T. C.; Blunt, N. S.; Booth, G. H.; Guo, S.; Li, Z.; Liu, J.; McClain, J. D.; Sayfutyarova, E. R.; Sharma, S.; et al. PySCF: the Python-based simulations of chemistry framework. *Wiley Interdiscip. Rev.: Comput. Mol. Sci.* **2018**, *8*, No. e1340.
(29) Wang, L.-P.; Song, C. Geometry optimization made simple with translation and rotation coordinates. *J. Chem. Phys.* **2016**, *144*, 214108.
(30) https://github.com/jhrmnn/pyberny (accessed December 1, 2019).
(31) Werner, H.-J.; Knowles, P. J.; Knizia, G.; Manby, F. R.; Schütz, M. Molpro: a general-purpose quantum chemistry program package. *WIRE Comput. Mol. Sci.* **2012**, *2*, 242.
(32) Xu, Z.; Luo, N.; Federman, S. R.; Jackson, W. M.; Ng, C.-Y.; Wang, L.-P.; Crabtree, K. N. Ab Initio Study of Ground-state CS Photodissociation via Highly Excited Electronic States. *Proceedings of the 74th International Symposium on Molecular Spectroscopy*, 2019; Vol. *882*, p 86.
(33) Mao, R.-Z.; Guo, F.; Xiong, D.-C.; Li, Q.; Duan, J.; Ye, X.-S. Photoinduced C-S Bond Cleavage of Thioglycosides and Glycosylation. *Org. Lett.* **2015**, *17*, 5606.
(34) Ganguly, T.; Majumdar, A. Comparative Study for the Cobalt(II)- and Iron(II)-Mediated Desulfurization of Disulfides Demonstrating That the C-S Bond Cleavage Step Precedes the S-S Bond Cleavage Step. *Inorg. Chem.* **2020**, *59*, 4037.
(35) Ashfold, M. N. R.; Bain, M.; Hansen, C. S.; Ingle, R. A.; Karsili, T. N. V.; Marchetti, B.; Murdock, D. Exploring the dynamics of the photoinduced ring-opening of heterocyclic molecules. *J. Phys. Chem. Lett.* **2017**, *8*, 3440.
(36) Roberts, G. M.; Stavros, V. G. The role of $\pi\sigma^*$ states in the photochemistry of heteroaromatic biomolecules and their subunits: insights from gas-phase femtosecond spectroscopy. *Chem. Sci.* **2014**, *5*, 1698.
(37) King, G. A.; Oliver, T. A. A.; Ashfold, M. N. R. Dynamical insights into $\pi 1\sigma^*$ state mediated photodissociation of aniline. *J. Chem. Phys.* **2010**, *132*, 214307.
(38) Roberts, G. M.; Williams, C. A.; Young, J. D.; Ullrich, S.; Paterson, M. J.; Stavros, V. G. Unraveling ultrafast dynamics in photoexcited aniline. *J. Am. Chem. Soc.* **2012**, *134*, 12578.

https://dx.doi.org/10.1021/acs.jpca.0c07593
J. Phys. Chem. A 2020, 124, 8273−8279

(39) Wang, F.; Neville, S. P.; Wang, R.; Worth, G. A. Quantum dynamics study of photoexcited aniline. *J. Phys. Chem. A* **2013**, *117*, 7298.
(40) Jhang, W. R.; Lai, H. Y.; Lin, Y.-C.; Lee, C.; Lee, S.-H.; Lee, Y.-Y.; Ni, C.-K.; Tseng, C.-M. Triplet vs $\pi\sigma^*$ state mediated N-H dissociation of aniline. *J. Chem. Phys.* **2019**, *151*, 141101.
(41) Druzhinin, S. I.; Ernsting, N. P.; Kovalenko, S. A.; Lustres, L. P.; Senyushkina, T. A.; Zachariasse, K. A. Dynamics of ultrafast intramolecular charge transfer with 4-(dimethylamino) benzonitrile in acetonitrile. *J. Phys. Chem. A* **2006**, *110*, 2955.
(42) Sobolewski, A. L.; Domcke, W. Promotion of intramolecular charge transfer in dimethylamino derivatives: twisting versus acceptor-group rehybridization. *Chem. Phys. Lett.* **1996**, *259*, 119.
(43) Sobolewski, A. L.; Domcke, W. Charge transfer in amino-benzonitriles: do they twist? *Chem. Phys. Lett.* **1996**, *250*, 428.
(44) Rotkiewicz, K.; Grellmann, K. H.; Grabowski, Z. R. Reinterpretation of the anomalous fluorescense of p-n,n-dimethylamino-benzonitrile. *Chem. Phys. Lett.* **1973**, *19*, 315.

https://dx.doi.org/10.1021/acs.jpca.0c07593
J. Phys. Chem. A 2020, 124, 8273−8279